New Phytologist

Research

A trade-off between leaf water retention capacity and rehydration capacity among plant species

Junzhou Liu[1,2], Tingting Du[1], Xianke Yang[1], Jinfang Zhao[1], Sheng Liang[1], Zhuo Chen[1], Hui Zhang[1], Yang Xiao[1] and Dongliang Xiong[1]

[1]National Key Laboratory of Crop Genetic Improvement, Hubei Hongshan Laboratory, MARA Key Laboratory of Crop Ecophysiology and Farming System in the Middle Reaches of the Yangtze River, Huazhong Agricultural University, Wuhan, Hubei, 430070, China; [2]Center for Agricultural Water Research in China, China Agricultural University, No. 17 Qinghua East Road, Haidian District, Beijing, 100083, China

Author for correspondence:
Dongliang Xiong
Email: dlxiong@mail.hzau.edu.cn

Received: *30 April 2025*
Accepted: *15 November 2025*

New Phytologist (2025)
doi: 10.1111/nph.70821

Key words: cell size, Chl fluorescence, drought avoidance, drought resistance strategies, drought tolerance, minimum leaf conductance, succulent.

Summary

- How plants cope with drought remains a major challenge in plant biology. Plants have evolved diverse drought resistance strategies, whether they operate synergistically or exhibit trade-offs remains a critical knowledge gap.
- Here, we examined drought resistance strategies across 128 plant species, encompassing diverse plant phyla, original biomes, leaf types, and growth forms. Their leaf water retention capacity, rehydration capacity, and anatomical traits of leaves were measured.
- Our analyses revealed a significant negative correlation between leaf water retention capacity and rehydration capacity ($R^2 = 0.55$, $P < 0.001$), providing compelling evidence for an trade-off between desiccation avoidance and desiccation tolerance at the leaf level. This trade-off exhibits clear anatomical underpinnings in leaf structural traits including cell size, leaf thickness, vein density, and xylem proportion. We found significant variations in both capacities across plant phyla, original biomes, and leaf types, suggesting that vascular structure evolution and habitat adaptation may be primary drivers shaping drought resistance strategies. Notably, interspecific differences in leaf water retention capacity were mainly due to variations in water loss rate rather than water storage capacity.
- Our findings advance mechanistic understanding of drought resistance strategies across different plant types and contribute to improved predictions of vegetation responses to climate change.

Introduction

Drought has emerged as an important abiotic stressor driving global forest mortality and destabilizing ecosystem functions across biomes (Allen *et al.*, 2010), and climate change amplifies its frequency and severity in recent years (IPCC, 2023). However, understanding how plants cope with drought remains a major challenge in plant ecology. Plants employ three primary drought resistance strategies: maintaining high tissue water content through water conservation and acquisition (avoidance), tolerating low tissue water content (tolerance), and accelerating reproduction before stress onset (escape) (Levitt, 1980; Gupta *et al.*, 2020). However, whether these strategies operate synergistically or exhibit trade-offs remains a critical knowledge gap (Liang & Ye, 2024). Resolving these interactions is essential for advancing our understanding of vegetation distribution and predicting the succession of plant communities under climate change.

Resource allocation theory suggests potential trade-offs between drought resistance strategies (Reich & Cornelissen, 2014). This idea is supported by extensive studies in natural systems that have documented trade-offs between drought avoidance and tolerance across species (Pineda-Garcia *et al.*, 2013; Christoffersen *et al.*, 2016; Bristiel *et al.*, 2018; Fallon & Cavender-Bares, 2018; Forner *et al.*, 2018; Chen *et al.*, 2020; Díaz-Castellanos *et al.*, 2022; Ziegler *et al.*, 2024). However, such trade-offs are not consistently observed in all studies (Nadal *et al.*, 2021, 2023; Andrade *et al.*, 2024). The lack of consensus may arise from two major sources. First, the inherent complexity of whole-plant systems, where compensatory interactions among different organs may obscure the trade-off at the plant level. Second, the limited taxonomic and geographic scope of existing research, which often focuses on few species or particular regions, potentially leading to sampling bias and inflated conclusions about generality. To address these issues, this study focuses on leaves, the primary site of water loss and a key vulnerability point under drought, and examines a broad range of species to improve the generalizability and mechanistic clarity of drought resistance trade-offs.

Multiple lines of evidence from ecological studies suggest the existence of an avoidance-tolerance trade-off at the leaf level.

Latitudinal patterns reveal consistent differences in drought strategies – low-latitude plants exhibit enhanced desiccation avoidance through reduced minimum leaf conductance (g_{min}, refer to Supporting Information Table S1 for the list of abbreviations) (Duursma *et al.*, 2018), enabling better control of water loss, yet show markedly decreased tolerance evidenced by greater vulnerability to both rehydration failure and loss of Chl fluorescence during dehydration (John *et al.*, 2018; Fortunel *et al.*, 2023). This trade-off is further illustrated by contrasting plant groups that have evolved under different moisture regimes: moisture-loving mosses have evolved remarkable abilities to recover from near-complete desiccation despite poor water retention capacity (Proctor & Tuba, 2002), while desert-dwelling succulents have developed extensive adaptations for water retention but cannot survive severe dehydration (Fradera-Soler *et al.*, 2022). Additionally, the shift in dominant vegetation from high-tolerance to high-avoidance species along increasing aridity gradients suggests that environmental conditions drive the evolution of these contrasting strategies (Aguilar-Romero *et al.*, 2017; Kramp *et al.*, 2022).

The structural basis underlying this trade-off appears to be rooted in leaf cellular architecture and development. Research has demonstrated that smaller cell volumes enhance desiccation tolerance by reducing membrane damage during cell contraction under water stress (Cutler *et al.*, 1977; Turner, 1986; Ding *et al.*, 2014). However, evolutionary coordination between cell size, vein architecture, and stomatal development means that leaves with smaller cells typically develop higher vein density and greater gas exchange capacity (Brodribb *et al.*, 2013; Scoffoni *et al.*, 2016). While these traits can enhance resource acquisition and growth potential, they often come at the cost of reduced water retention ability (Machado *et al.*, 2020; S Wang *et al.*, 2024). This fundamental link between cellular architecture and physiological function may explain why plants cannot simultaneously maximize both avoidance and tolerance strategies.

Characterizing these drought adaptation strategies requires careful consideration of multiple physiological indicators. Water retention capacity, measured through changes in relative water content over time (Fig. S1a), serves as a key metric for desiccation avoidance (Clarke & McCaig, 1982; Muchow & Sinclair, 1989; Cameron *et al.*, 2006; Zhu & Xiong, 2013; Wang *et al.*, 2023; J. Wang *et al.*, 2024). This capacity depends on both g_{min} after stomatal closure and intrinsic water storage ability. Although both low g_{min} and high water storage ability contribute to the maintenance of high leaf water content, their relative contributions to interspecific variation remain poorly understood. For assessing tolerance, both rehydration capacity (Fig. S1b) (Bajji *et al.*, 2002; Trifilo *et al.*, 2023) and Chl fluorescence retention (Fig. S1c) (Maxwell & Johnson, 2000; Baker, 2008; Song & Zhu, 2024) during dehydration provide critical insights, with recent evidence suggesting that loss of rehydration capacity – a lethal condition – typically precedes Chl fluorescence decline (John *et al.*, 2018; Trueba *et al.*, 2019; Fortunel *et al.*, 2023; Wang *et al.*, 2023).

We hypothesized that the universality of leaf-level avoidance-tolerance trade-offs exists among plant species. Accordingly, leaf water retention capacity, rehydration capacity and Chl fluorescence during dehydration, and anatomical underpinnings across 128 plant species, representing diverse phyla, original biomes, growth forms, and leaf types (refer to Table S2 for detailed species information), were investigated. Additionally, we analyzed how g_{min} and water storage capacity contribute to interspecific variation in leaf water retention. This comprehensive approach allows us to evaluate fundamental constraints on drought adaptation strategies across major plant lineages while illuminating their structural and physiological bases.

Materials and Methods

Plant materials

This study analyzed a diverse set of 128 plant species spanning multiple phyla, including bryophytes, ferns, gymnosperms, and angiosperms. These species originated from a wide range of biomes, covering tropical, subtropical, temperate, arid, and humid habitats. The collection also included different growth forms, such as woody and herbaceous plants, and varied leaf types, including evergreen, deciduous, annual, and perennial species, as detailed in Table S2. Among these species, 97 were naturally grown on the campus of Huazhong Agricultural University (N 30°47', E 114°36', altitude 37 m) or in the nearby Qinglongshan National Forest Park, located *c.* 16 km away. Meanwhile, 21 species were cultivated outdoors in pots or under shaded conditions due to their specific habitat requirements, and they were regularly irrigated. Additionally, 10 moss species were grown in transparent plastic boxes to maintain high relative humidity. All species cultivated in pots or boxes were categorized as tropical or temperate plants and were not native to the region.

Leaf sampling for most species took place from July to September in 2022, 2023, and 2024, while moss sampling was conducted in May and June to avoid the adverse effects of high summer temperatures on moss growth. For each species, leaves were collected in the morning from at least three individual plants. To minimize the potential influence of leaf age, only current-year leaves were sampled for evergreen woody and perennial herbaceous species.

Desiccation curves

To generate complete desiccation curves, leaves were first rehydrated. For larger plants, branches were sampled, and their cut ends were submerged underwater after being recut. Care was taken to ensure that only the cut ends were submerged and that the leaves remained at least 10 cm above the water surface. For small herbaceous species, whole plants with roots were collected, and only the roots were submerged for rehydration. This process was conducted in the dark for 1–3 h, until the leaf water potential, determined using a pressure chamber (Model 3005; Soilmoisture Equipment Corp., USA), exceeded −0.3 MPa. Moss samples were prepared by growing them under water-saturated conditions, and surface water was carefully removed using tissues to obtain fully hydrated samples.

Following rehydration, five detached leaf or moss samples were dried on a bench in a dark environment to establish dehydration curves. The experiments were conducted in a room maintained at 29°C with 60% relative humidity. Leaf weight changes were periodically measured using an analytical balance (MS205DU; Mettler Toledo, Columbus, OH, USA). At the start of the experiment, leaves were scanned to measure their leaf area (A_{leaf}, mm^2), and at the end, they were oven-dried to obtain their dry weight (DW, g). Desiccation curves were constructed by plotting relative water content (RWC, %) against time (t, h). The RWC was calculated as follows:

$$RWC = (W_i - DW)/(W_0 - DW) \quad \text{Eqn 1}$$

where W_0 is the turgid leaf weight at beginning and W_i is the leaf weight recorded at the i time.

The leaf saturated water content (SWC, g H_2O g^{-1} DW) was calculated as

$$SWC = (W_0 - DW)/DW \quad \text{Eqn 2}$$

The area of a single leaf (LA, cm^2) was measured using images scanned for A_{leaf}. However, LA measurements were not conducted for compound-leaf species, mosses, and conifers because of the challenge in accurately identifying their individual leaves.

The leaf mass per area (LMA, g cm^{-2}) was calculated as

$$LMA = DW/A_{leaf} \quad \text{Eqn 3}$$

The leaf dry matter content (LDMC) was calculated as

$$LDMC = DW/W_0 \quad \text{Eqn 4}$$

The leaf vapor conductance (mmol m^{-2} s^{-1}) during desiccation was calculated as follows:

$$\text{Leaf vapor conductance} = \frac{\frac{W_i - W_{i+1}}{t_{i+1} - t_i} \times p_a}{A_{leaf} \times VPD \times m_{H2O}} \quad \text{Eqn 5}$$

where VPD is the vapor pressure deficit (kPa) according to the temperature and the relative humidity recorded; p_a is the atmospheric pressure (101.6 kPa); m_{H2O} is the molecular mass of H_2O (18 g mol^{-1}); W_i and t_i are the leaf weight (g) and time (h) recorded at the i time, respectively. According to the leaf conductance vs RWC curve, the leaf conductance was relatively constant between 40 and 70% RWC in most species (see the Results section), thus the minimum leaf conductance (g_{min}, mmol m^{-2} s^{-1}) was calculated as the average of leave vapor conductance between which.

Rehydration curves

Branches or plants were sampled and rehydrated using the same protocol in the leaf dehydration process. For each species, a total of 35 leaves were prepared to determine the rehydration capacity. These leaves were desiccated to achieve varying RWC under the same room conditions in leaf desiccation curve measurements (dark, 29°C, and 60% RH); then leaf petioles were submerged in water for rehydration and placed in a sealed plastic box for 12 h. To attain optimal rehydration levels across all species, the rehydration time is longer than 8 h in some previous experiments, but this approach may lead to minor oversaturation issues for certain species (John *et al.*, 2018; Trifilo *et al.*, 2023). The saturated weight (W_s, g), pre-rehydration weight (W_d, g), post-12-h rehydration weight (W_r, g), and DW for each leaf were recorded. Then the percentage loss of rehydration capacity (PLRC, %) of each leaf was calculated as:

$$PLRC = \left(1 - \frac{W_r - W_d}{W_s - W_d}\right) \times 100\% \quad \text{Eqn 6}$$

Chloroplast fluorescence loss curves

Chloroplast fluorescence assessments were performed on the same samples used for determining leaf rehydration capacity. A pulse-modulated Chl fluorescence meter (Junior PAM, Walz, Germany) was used to measure the maximum quantum yield of the PSII (F_v/F_m) of leaves across different desiccation degrees before rehydration. Notably, before dehydration, each leaf was acclimated in the dark for 2 h, and was maintained under dark conditions throughout the subsequent dehydration process.

Leaf saturated osmotic potential

Branches or plants were sampled and rehydrated using the same protocol in leaf desiccation curve measurement. Subsequently, five leaf samples were individually sealed in tubes and stored at −70°C. A vapor-pressure osmometer (VAPRO5600; Wescor Inc., Logan, UT, USA) was used to measure the osmotic concentration of these samples. Then the leaf osmotic potential at full hydration (π_0, MPa) was calculated using the Van't Hoff equation (Liu *et al.*, 2023).

Leaf anatomy

Five leaves were randomly sampled from at least three individuals for each species. The blade tissues were excised from the central region of leaves and then were stored in FAA solution (-formalin/acetic acid/50% ethanol, 5/5/90, v/v/v) for 2–5 d. Standard paraffin sections were then prepared. Various anatomical parameters, including leaf thickness (LT, μm), upper epidermal thickness (UET, μm), lower epidermal thickness (LET, μm), total epidermal thickness (TET, μm) and its ratio to LT (ETR, %), palisade tissue thickness (PTT, μm) and its ratio to LT (PTR, %), spongy tissue thickness (STT, μm) and its ratio to LT (STR, %), vein density (VD, mm^{-2}), the proportion of xylem area to total cross-section area (XR, %), cell size (CS, μm^2), and mesophyll porosity (MP, %), were quantified using CaseViewer software (3DHISTECH Ltd, Budapest, Hungary) or Adobe Photoshop 2022 (Adobe Systems Inc., San Jose, CA, USA). The average cross-sectional area of epidermal cells, spongy tissue cells, and palisade tissue cells was determined in each leaf

sample by randomly selecting three cells per type. These averages were then weighted according to the proportional thickness of each tissue layer within the leaf to calculate the CS.

Statistical analyses

Turgor loss and leaf mortality have been consistently observed to occur *c.* 90% (Bartlett *et al.*, 2014) and 50–60% RWC (Mantova *et al.*, 2021; Trifilo *et al.*, 2023; Alon *et al.*, 2024), respectively, in most species. Therefore, the time for a 10% and a 50% loss of RWC (T_{RWC10} and T_{RWC50}, h) was linearly interpolated according to the adjacent points from leaf desiccation curves for evaluating desiccation avoidance.

The leaf rehydration curve was constructed by plotting PLRC against the RWC before rehydration. The logistic regression model was applied to fit the data points in SigmaPlot 12.5 (SPSS Inc., Chicago, IL, USA). Since traits with a sigmoid response curve typically exhibit a significant change after a loss of *c.* 10% of their maximum value (John *et al.*, 2018; Corso *et al.*, 2020; Creek *et al.*, 2020; Wang *et al.*, 2023), the RWC corresponding to a 10% reduction in rehydration capacity (RWC_{PLRC10}) was selected as the threshold for evaluating desiccation tolerance. The leaf chloroplast fluorescence loss curve was also constructed by plotting F_v/F_m against the RWC before rehydration. The logistic regression model was applied to fit the data points, similar to RWC_{PLRC10}, then the RWC threshold corresponding to a 10% loss of chloroplast fluorescence (RWC_{PLCF10}) was determined.

By using Spss 26.0 statistical software (SPSS Inc.), we conducted linear mixed effects models to analyze whether the leaf traits differed across categories, with plant phyla, biomes, growth forms, and leaf types as the fixed effects and the species as a random effect.

The correlation between traits was fitted using linear, sigmoidal, or Weibull functions in SigmaPlot 12.5.

Results

Quantifying water retention and rehydration capacities across species

We first characterized leaf water retention capacity across 128 plant species by measuring T_{RWC50}– the time required for a 50% loss of relative water content (RWC) from saturation. T_{RWC50} varied by several orders of magnitude among species, following a normal distribution in vascular plants (Fig. 1a). While bryophytes lost 50% of their RWC within just 15 min, exhibiting extremely low T_{RWC50} values, vascular plants (ferns, gymnosperms, and angiosperms) showed relatively higher and similar T_{RWC50} values (Fig. 1c). The range spanned from 0.08 h in the moss *Thuidium cymbifolium* Dozy & Molk to 2872.05 h in the succulent *Sansevieria trifasciata* Prain.

Water retention capacity showed clear biogeographic and ecological patterns. T_{RWC50} values decreased systematically from tropical to temperate regions and from arid to humid areas (Fig. 1d). Crops, analyzed separately due to their domestication history, exhibited the lowest T_{RWC50} among all groups. Leaf type also influenced water retention – perennial herbaceous plants maintained higher T_{RWC50} than annuals, and evergreen woody species exceeded deciduous species, though woody and herbaceous species showed no significant difference (Fig. 1e).

Leaf rehydration capacity, measured as RWC_{PLRC10} (the RWC threshold at 10% loss of rehydration capacity), also varied substantially across species (Fig. 1b). Values ranged from 5.0% in the moss *Actinothuidium hookeri* (Mitt.) Broth., indicating strong rehydration capacity, to 89.6% in the herbaceous angiosperm *Canna glauca* L. Like water retention, rehydration capacity showed significant variation across plant phyla, original biomes, leaf types, and growth forms (Fig. 1c–e), with woody species exhibiting notably higher RWC_{PLRC10} than herbaceous species.

The trade-off between leaf water retention and rehydration capacities

Our analysis revealed a significant negative correlation between T_{RWC50} and RWC_{PLRC10} across 128 plant species (Fig. 2a), supporting our initial hypothesis. This trade-off between leaf water retention and rehydration capacities remained significant across different original biomes (Fig. 2c) and leaf types (Fig. 2d), though it was not significant across different plant phyla (Fig. 2b).

We also quantified RWC thresholds at 10% loss of Chl fluorescence (RWC_{PLCF10}) to evaluate leaf desiccation tolerance. The results demonstrated that rehydration capacity loss preceded Chl fluorescence loss during dehydration in most species, with exceptions observed in three angiosperms and all nine mosses (Fig. 1b). No significant correlation was detected between T_{RWC50} and RWC_{PLCF10} across species (Fig. S2).

The critical role of cell size in this trade-off

To elucidate the mechanisms underlying this trade-off, we examined leaf anatomical and physiological traits. Cell size (CS) emerged as the most significant trait, with our analysis revealing strong correlations between CS, leaf thickness (LT), vein density (VD), and the ratio of xylem area to total leaf cross-sectional area (XR) with both leaf water retention and rehydration capacities ($R^2 = 0.24$–0.69, $P < 0.001$) (Fig. 3). CS demonstrated robust coordination with LT, VD, and XR ($R^2 = 0.64$–0.76, $P < 0.001$) (Fig. S3). Both leaf capacities also correlated with epidermal thickness (ET) and spongy tissue thickness (STT) ($R^2 = 0.10$–0.42, $P < 0.001$), as LT comprises various tissue thicknesses. Weaker correlations were observed between these leaf capacities and saturated water content (SWC), leaf mass per area (LMA), and tissue thickness proportions ($R^2 = 0.07$–0.29, $P < 0.001$) (Fig. S3). Notably, increasing epidermal tissue proportion showed opposite effects on these leaf capacities compared to increases in palisade and sponge tissue proportions.

Several traits, including leaf dry matter content (LDMC), single leaf area (LA), saturated osmotic potential (π_0), and mesophyll porosity (MP), showed no significant correlations with either leaf capacity, suggesting they do not mediate this trade-off (Fig. S3).

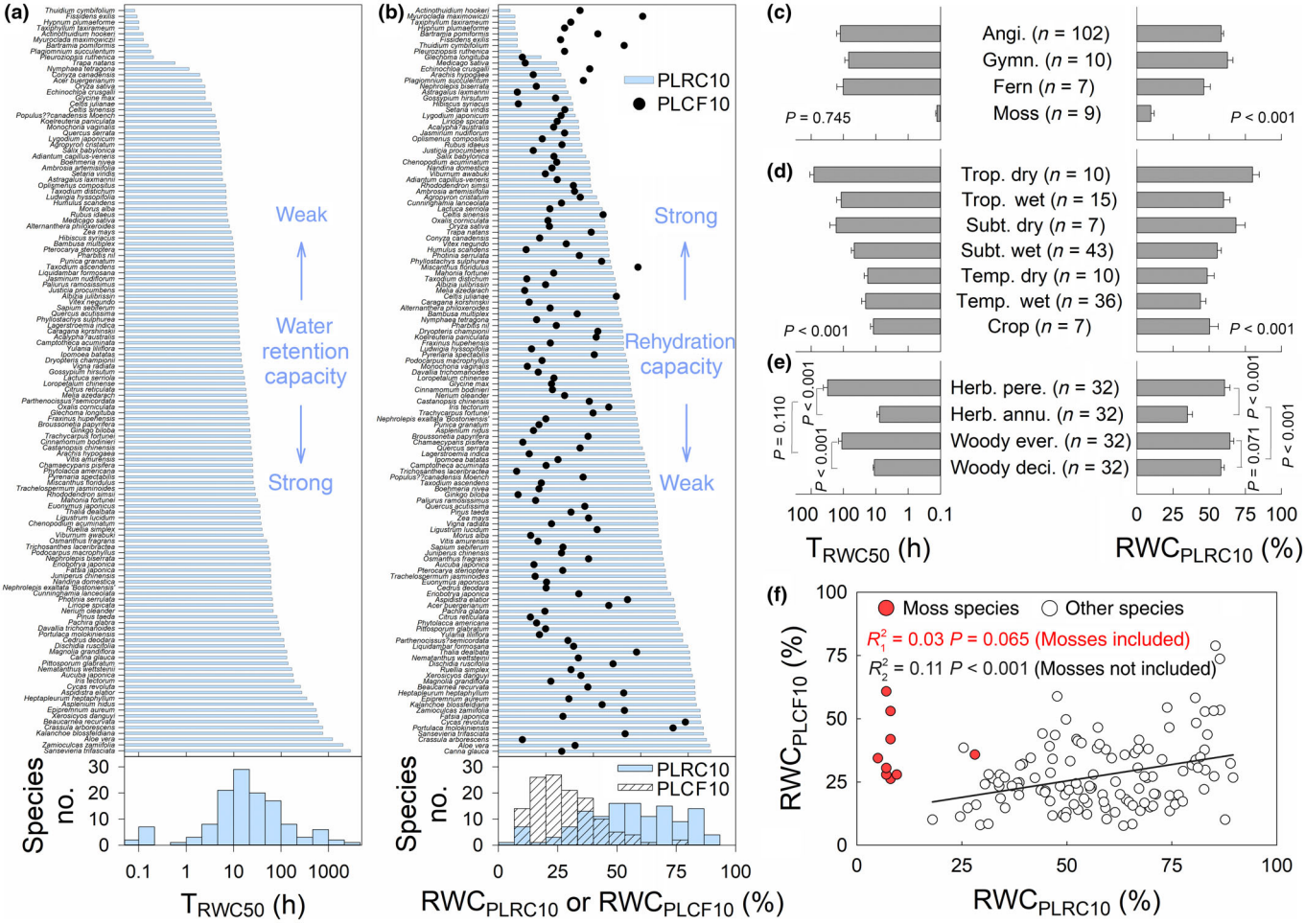

Fig. 1 Diversities of leaf water retention capacity, rehydration capacity, and chlorophyll fluorescence retention capacity across 128 species. Values of (a) T_{RWC50} and (b) RWC_{PLRC10} and RWC_{PLCF10} of each species and their distributions. Differences in T_{RWC50} and RWC_{PLRC10} across (c) plant phyla, (d) original biomes, and (e) growth forms and leaf types. (f) The relationship between RWC_{PLRC10} and RWC_{PLCF10}, with regression lines and statistical significance (R^2 and P-values). T_{RWC50}, the time for a 50% loss of relative water content from saturation; RWC_{PLRC10}, the relative water content at a 10% loss of rehydration capacity; RWC_{PLCF10}, the relative water content at a 10% loss of chlorophyll fluorescence. Angi., angiosperm; annu., annual; deci., deciduous; ever., evergreen; Gymn., gymnosperm; Herb., herbaceous; pere, perennial; Subt., subtropical; Temp., temperate; Trop., tropical. In (a, b, f), values are means for each species, $n = 5$; in (c–e), values are means ± SE. PLRC, percentage loss of rehydration capacity; RWC, relative water content.

Minimum leaf conductance dominate the variation in leaf water retention capacity across species

Under dark conditions, we measured complete dehydration curves from 100% RWC to near 0%. Most species exhibited declining leaf vapor conductance with decreasing RWC, making it challenging to identify stable conductance ranges despite controlled measurement conditions (Fig. 4a). We observed four distinct response patterns: (1) initial conductance decrease followed by a plateau with a clear inflection point, most common across species (Fig. 4b); (2) initially stable conductance, typical in evergreen woody species (Fig. 4c); (3) continuous conductance decline without stability, characteristic of mosses, floating plants, and leaf-curling species (Fig. 4d); and (4) initially stable conductance with sharp increases at critical RWC points, typical of succulent plants (Fig. 4e). We defined g_{min} as the average conductance within the 40–70% RWC range, where conductance remained relatively stable across species.

Given that leaf water loss rate and water storage capacity primarily affect T_{RWC50} variation (Blackman *et al.*, 2016), we analyzed the contributions of minimum leaf conductance (g_{min}) and SWC. Our analysis demonstrated a strong correlation between T_{RWC50} and g_{min} across species (Fig. 4f; $R^2 = 0.81$, $P < 0.001$), whereas the correlation with SWC was relatively weak (Fig. 4g; $R_1^2 = 0.21$, $P < 0.001$). Notably, excluding succulent plants eliminated any significant correlation between T_{RWC50} and SWC (Fig. 4g; $R_2^2 = 0.03$, $P = 0.079$).

Discussion

Our research demonstrated a significant negative correlation between leaf water retention and rehydration capacities across

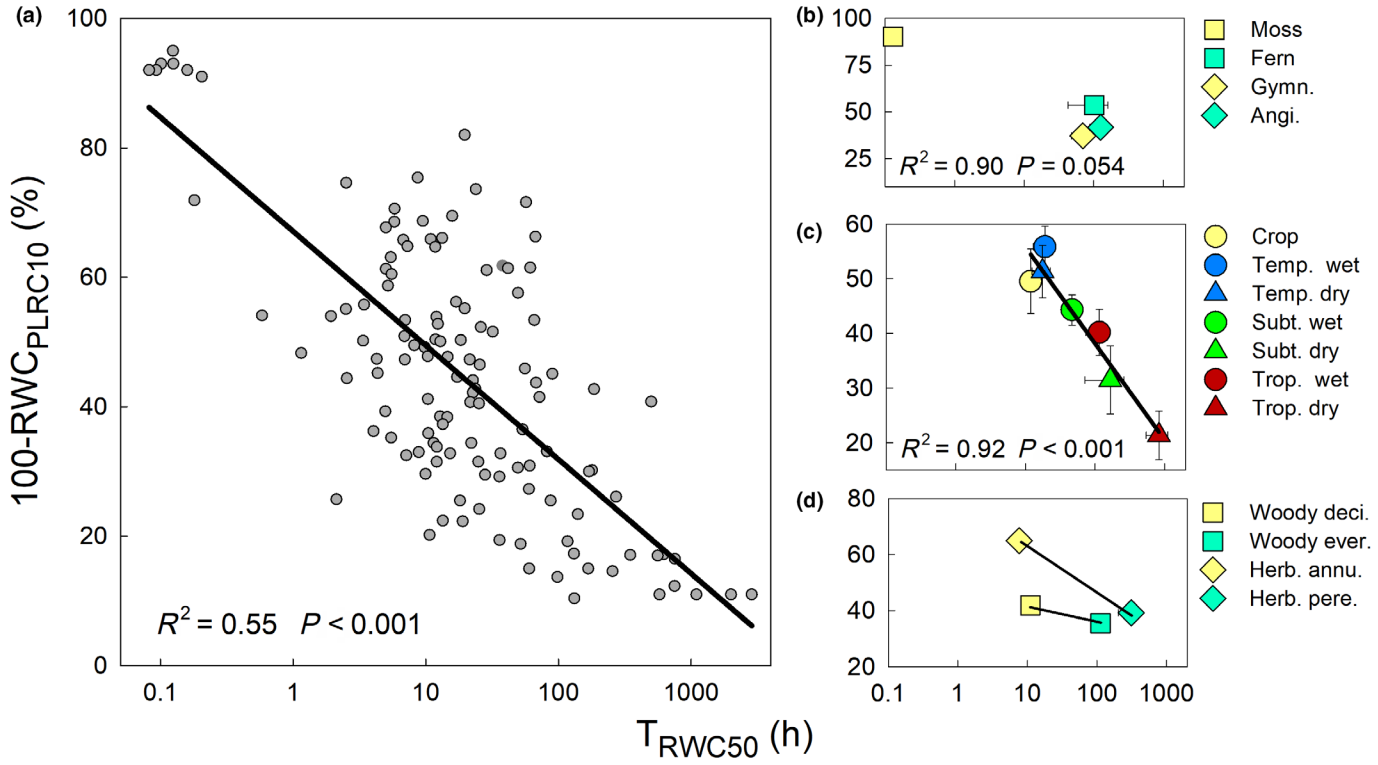

Fig. 2 The significant negative correlation between leaf water retention capacity and rehydration capacity across 128 species. Data are presented on (a) species, (b) plant phyla, (c) original biomes, and (d) growth forms and leaf types. T_{RWC50}, the time for a 50% loss of relative water content from saturation; RWC_{PLRC10}, the relative water content at a 10% loss of rehydration capacity. Angi., angiosperm; annu., annual; deci., deciduous; ever., evergreen; Gymn., gymnosperm; Herb., herbaceous; pere, perennial; Subt., subtropical; Temp., temperate; Trop., tropical. In (a), values are means for each species, $n = 5$; in (b–d), values are means ± SE. PLRC, percentage loss of rehydration capacity; RWC, relative water content.

128 plant species (Fig. 2a). This finding substantiates the hypothesized trade-off between desiccation avoidance and desiccation tolerance strategies at the leaf level across species.

The water retention capacity (Riederer & Schreiber, 2001; Sampangi-Ramaiah *et al.*, 2016) and rehydration capacity (John *et al.*, 2018; Trifilo *et al.*, 2023; Liu *et al.*, 2024b) of leaves, governed by distinct physiological mechanisms, appears independent. However, anatomical analyses revealed an inherent link, with cell size (CS) as the critical trait mediating this trade-off. Leaves with strong water retention but weak rehydration capacity typically exhibit larger CS, lower vein density (VD), lower ratio of xylem area to total leaf cross-sectional area (XR), and higher leaf thickness (LT) (Fig. 3). Conversely, leaves with weak water retention but strong rehydration capacity show opposing traits. The loss of rehydration capacity during dehydration is primarily due to mechanical damage to cell membranes (John *et al.*, 2018; Azzara *et al.*, 2022). Smaller CS mitigates such damage by reducing dehydration-induced cell shrinkage, enhancing desiccation tolerance (Cutler *et al.*, 1977; Turner, 1986). Given the coevolution of CS and VD (Brodribb *et al.*, 2013), we found strong negative correlations between CS and both VD and XR (Fig. S3). Increased VD and XR can buffer dehydration-induced damage by facilitating water release from conduits to mesophyll, improving hydraulic conductivity and gas exchange (Holtta *et al.*, 2009). Moreover, a positive correlation between minimum leaf conductance (g_{min}) and maximum stomatal conductance indicates low water retention in these plants (Machado *et al.*, 2020; S. Wang *et al.*, 2024). Our findings align with studies showing that higher epidermal tissue proportions enhance rehydration capacity but reduce water retention (Fig. S3), while variations in palisade and sponge tissue have the opposite effect (Oppenheimer & Leshem, 1966). Leaf mass per area (LMA) and saturated water content (SWC) are also linked to this trade-off (Fig. S3), although our LMA results differ from previous findings (John *et al.*, 2018). These insights highlight the anatomical basis of the water retention–rehydration trade-off.

The evolution of vascular systems likely drives this trade-off. Early land colonizers like mosses and lichens lacked a waxy epidermis and had weak water retention but could quickly resume metabolism after rewetting (Smith & Molesworth, 1973; Sancho & Kappen, 1989). The advent of vascular systems, epidermis, and stomata marked a pivotal evolutionary shift. Most vascular plants have since lost desiccation tolerance but diversified their drought resistance strategies, adapting to complex environments (Alpert, 2006). While methods such as phylogenetic independent contrasts provide powerful tools for addressing such questions (Brodribb *et al.*, 2014; Scoffoni *et al.*, 2016; Xiong & Flexas, 2020), their application across deeply divergent lineages,

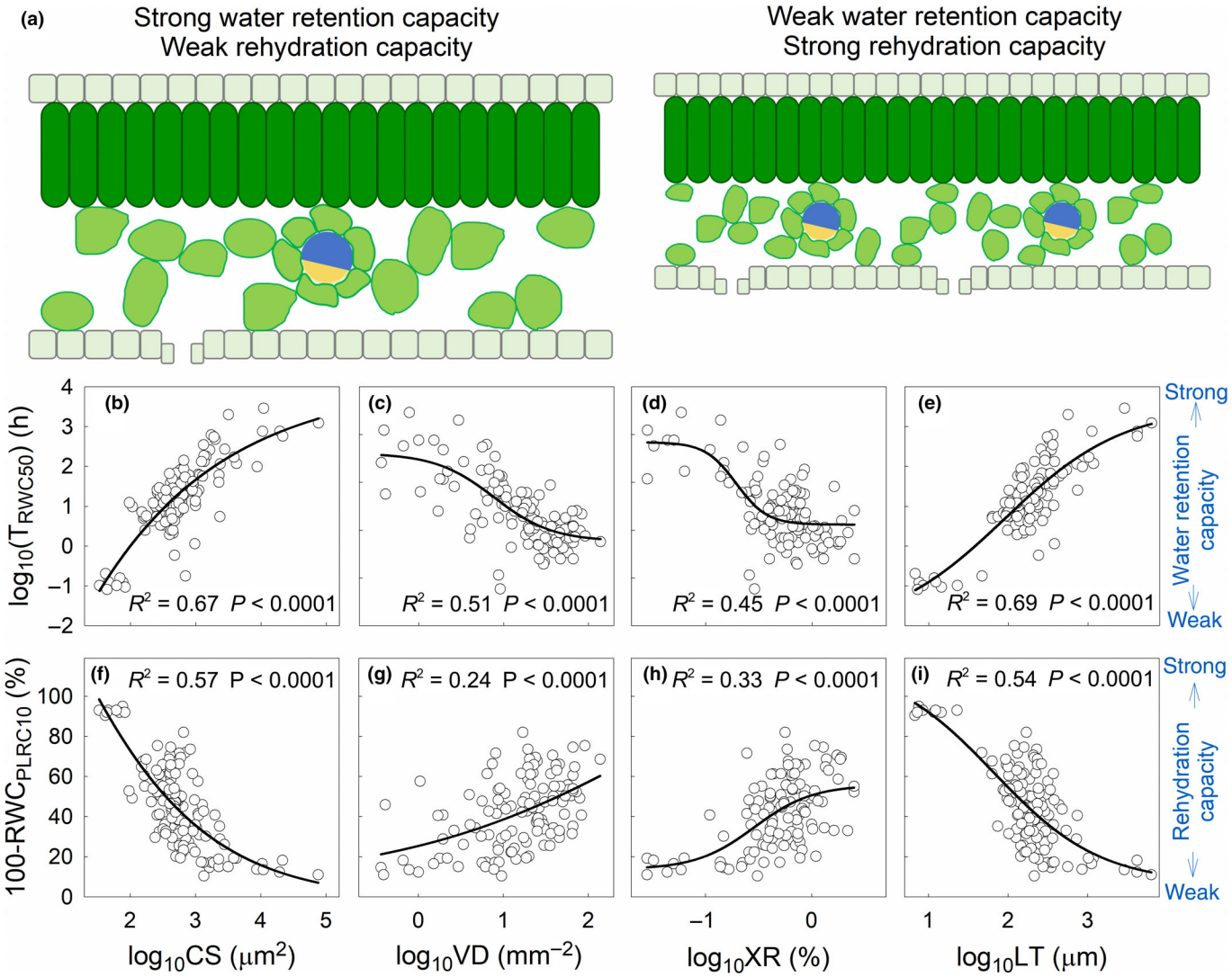

Fig. 3 The close relationship between leaf anatomies and leaf water retention capacity and rehydration capacity across 128 species. (a) A schematic of two leaf structures possessing different water retention capacities and different rehydration capacities. The correlations between cell size, vein density, xylem proportion, and leaf thickness with (b–e) leaf water retention capacity and (f–i) rehydration capacity, with regression lines and statistical significance (R^2 and *P*-values). T_{RWC50}, the time for a 50% loss of relative water content from saturation; RWC_{PLRC10}, the relative water content at a 10% loss of rehydration capacity. CS, cell size; PLRC, percentage loss of rehydration capacity; LT, leaf thickness; RWC, relative water content; VD, vein density; XR, ratio of xylem area to total leaf cross-sectional area. Values are means for each species, $n = 5$.

including bryophytes, ferns, and gymnosperms, remains challenging. Future studies employing robust phylogenetic frameworks could offer further insights into the evolutionary dynamics of this trade-off. External factors, such as habitat temperature and drought levels, may be another driving force. Tropical plants tend to have high water retention but low rehydration capacities, whereas temperate plants show the opposite. This pattern aligns with the distribution of evergreen woody and perennial herbaceous plants in tropical regions and deciduous and annual plants in temperate areas (Fig. S4) (Wright *et al.*, 2004), and with their LMA (Fig. S5), reflecting resource conservation vs acquisition strategies (Reich & Cornelissen, 2014). Temperate plants, which exhibit greater cold tolerance, often adapt through synergistic traits like freezing and desiccation tolerance (Holmlund, 2021). In arid biomes, vegetation shifts from desiccation-tolerant to desiccation-avoidant species as drought intensity increases (Aguilar-Romero *et al.*, 2017; Kramp *et al.*, 2022), supporting the observed trade-offs.

Leaf water retention and rehydration capacities exhibit environmental plasticity, yet interspecific differences overwhelmingly dominate over plastic response. Although environmental factors, such as temperature, soil water, and salinity, can significantly affect g_{min} (Duursma *et al.*, 2018; Lopez *et al.*, 2021; Challis *et al.*, 2022; Liu *et al.*, 2023), a key trait associated with leaf water retention, the extent of plasticity is relatively small (generally < 3-fold) compared to the orders-of-magnitude variation

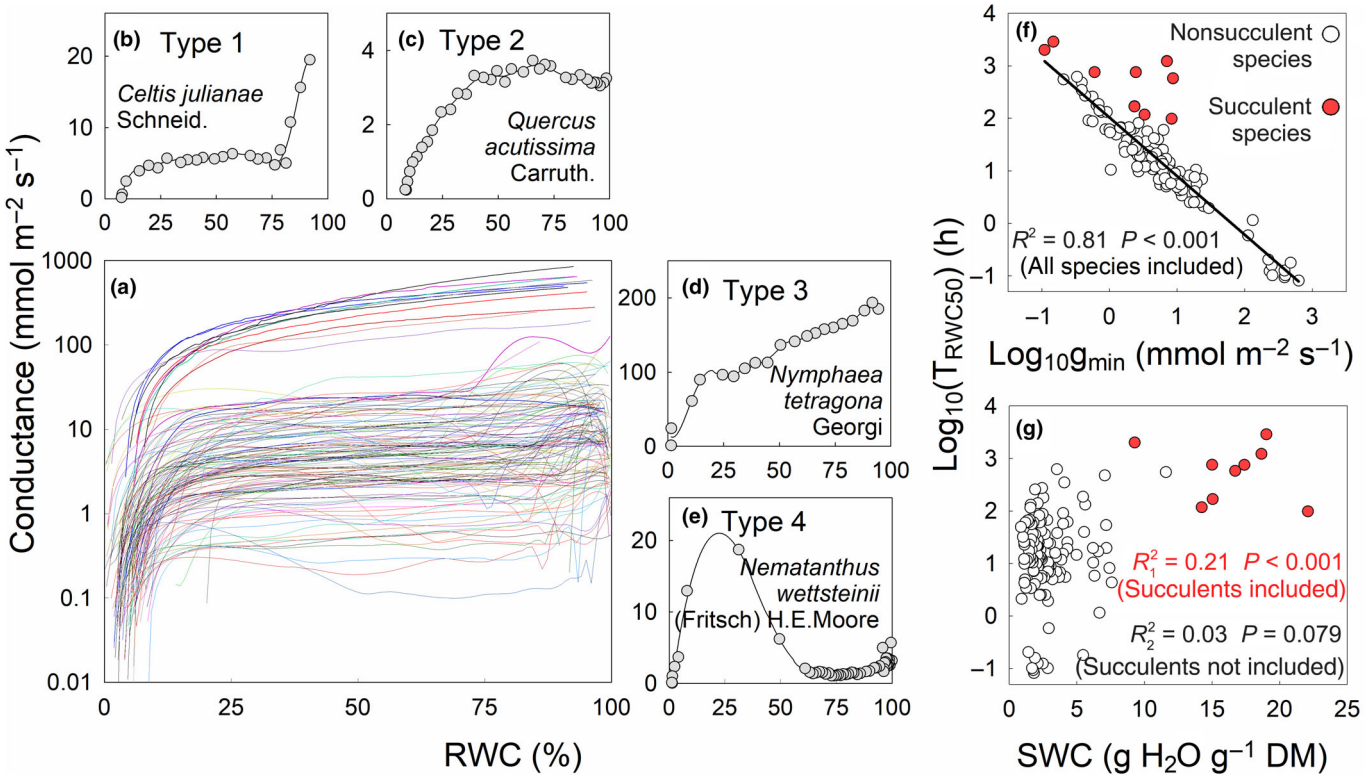

Fig. 4 Factors impacting the leaf vapor conductance or water retention capacity among species. (a) Leaf dehydration curves of the 128 species. (b–e) Four typical types of leaf dehydration curves; the Latin names of the representative species are displayed. Correlations between leaf water retention capacity and (f) minimum leaf conductance (g_{min}) and (g) saturated water content (SWC) among species, with regression lines and statistical significance (R^2 and *P*-values). T_{RWC50}, the time for a 50% loss of relative water content from saturation. In (a–e), each curve represents a smoothed fit of data points showing the temporal change in leaf vapor conductance for a single species; in (f, g), values are means for each species, $n = 5$. RWC, relative water content.

observed among species (Fig. 4f). Similarly, plasticity in cell size, a critical anatomical trait mediating this trade-off, is also constrained (generally < 3-fold; Binks *et al.*, 2016; Liu *et al.*, 2024a; Khoma & McAdam, 2025; Raza *et al.*, 2025; Samantara *et al.*, 2025), and much smaller than the extensive interspecific variation (Fig. 3b). Moreover, leaf rehydration capacity shows only minor or statistically insignificant responses to environmental change (Burghardt *et al.*, 2008; Li *et al.*, 2020; Guo *et al.*, 2023). Therefore, although differences in sampling years or growing conditions (potted or wild) may influence leaf water retention and rehydration capacities, it is unlikely that such effects would undermine the conclusion that a trade-off exists between these two capacities.

We quantified two key indicators, RWC_{PLRC10} and RWC_{PLCF10}, to assess leaf desiccation tolerance. Our results show that rehydration capacity loss precedes F_v/F_m loss during dehydration in most species, except for some tropical trees, as they had the highest RWC_{PLCF10} (Fig. S6), indicating that rehydration capacity is a better marker of desiccation tolerance and post-drought recovery. This functional decline sequence aligns with observations reported in most angiosperms (John *et al.*, 2018; Trueba *et al.*, 2019; Fortunel *et al.*, 2023; Wang *et al.*, 2023). Bryophytes and certain vascular 'resurrection plants' display rapid rehydration and robust F_v/F_m retention, highlighting their adaptive advantages (Marks *et al.*, 2024). However, most vascular plants have low RWC_{PLCF10} relative to RWC_{PLRC10}, suggesting a limited role for F_v/F_m loss in assessing desiccation tolerance. Besides, it should be noted that the recovery of water content, while necessary, may not be sufficient for full physiological recovery. Damage to photosynthetic components or biochemical processes, not captured by F_v/F_m alone, and plant hydraulics, could impair gas exchange and carbon assimilation even after rehydration (Rehschuh *et al.*, 2020; Bi *et al.*, 2023; Wagner *et al.*, 2023; Zait *et al.*, 2024; Liu *et al.*, 2024b). Therefore, a more comprehensive evaluation including additional Chl fluorescence and gas exchange parameters may better capture drought stress responses.

Although g_{min} is widely recognized as a critical trait for drought resistance (Kerstiens, 1996; Duursma *et al.*, 2018; Blackman *et al.*, 2019; Ziegler *et al.*, 2024), our findings suggest that its importance may be even greater than previously assumed. While both minimizing g_{min} and enhancing water storage capacity are considered effective strategies for avoiding desiccation (Blackman *et al.*, 2016; Christoffersen *et al.*, 2016; Liang & Ye, 2024), our findings highlight g_{min}, rather than SWC, as the primary determinant of leaf water retention capacity and thus plant survival under drought (Fig. 4f,g). This is reasonable as elevating SWC via LMA, MP, or LT is resource-intensive (Fig. S7), while reducing g_{min} through modifications in epicuticular wax chemistry is cost-effective (Anfodillo *et al.*, 2002; Bueno *et al.*, 2019b; Grünhofer *et al.*, 2023). In addition, physical

adaptations like leaf curling also influence g_{min} (Liu *et al.*, 2023; Wang *et al.*, 2023).

During dehydration, leaves typically exhibit high initial water loss rates, which then relatively stabilize beyond a certain RWC (Fig. 4b). Although this pattern is commonly reported, the inflection point between these phases remains poorly understood (Burghardt, 2003; Schuster *et al.*, 2016; Bueno *et al.*, 2019a; S. Wang *et al.*, 2024). While this inflection point shows no correlation with T_{RWC50}, it significantly affects T_{RWC10} (Fig. S8), suggesting that delayed stomatal closure impacts water retention at high RWC, a finding deserving further investigation. In most species, the water loss rate does not fully stabilize after the inflection point but continues to decline slowly, a phenomenon also recently documented by Burlett *et al.* (2025). This continued decline may result from a reduced evaporative surface or unsaturated air spaces beneath stomata. Consequently, measuring g_{min} at a fixed RWC, especially at high RWC, may underestimate the true leaf water retention capacity and thus drought survival evaluation, highlighting the importance of characterizing the entire leaf dehydration curve.

Conclusion

This study reveals a fundamental trade-off between leaf water retention and rehydration capacity across 128 plant species spanning diverse phyla, biomes, and growth forms, reflecting a functional compromise between desiccation avoidance and tolerance at the leaf level. This trade-off is underpinned by key anatomical traits, including cell size, leaf thickness, vein density, and xylem proportion. Significant variations in both capacities were observed across plant phyla, native biomes, and leaf types, indicating that the evolution of vascular structures and habitat adaptation may be major drivers in shaping drought resistance strategies. Furthermore, variation in leaf water retention capacity was found to be primarily governed by differences in water loss rate rather than water storage capacity. Overall, this work enhances the mechanistic understanding of drought resistance strategies and contributes to improved predictions of vegetation responses to climate change.

Acknowledgements

We thank Linna Zheng, Shunjin Zhu, Enhui Xu, Qila Sha, Dechao Shao, Yinhao Zhao, and Shun Zhu from Huazhong Agricultural University for their help in measuring leaf water retention and rehydration capacities. We thank Dr Zhenmei Wang from the MARA Key Laboratory of Crop Ecophysiology and Farming Systems research platform in the Middle Reaches of the Yangtze River for her invaluable technical support and assistance throughout our experiments. This study was funded by the National Natural Science Foundation of China (grant no. 52209053).

Competing interests

None declared.

Author contributions

DX and JL designed the research; JL, JZ, SL, ZC, HZ, and YX carried out the experiment; JL, DX, TD, and XY analyzed the data; JL wrote a preliminary version of the manuscript and DX contributed to manuscript revisions; all authors read and approved the final version of the manuscript.

ORCID

Tingting Du https://orcid.org/0000-0002-2314-9890
Junzhou Liu https://orcid.org/0000-0002-1532-7239
Dongliang Xiong https://orcid.org/0000-0002-6332-2627
Xianke Yang https://orcid.org/0000-0001-6045-546X
Jinfang Zhao https://orcid.org/0000-0001-5403-647X

Data availability

All data supporting the findings of this study are included in the main text and supporting information. The source data underlying Figs 1–4 are provided as a Source Data file (Dataset S1).

References

Aguilar-Romero R, Pineda-Garcia F, Paz H, González-Rodríguez A, Oyama K. 2017. Differentiation in the water-use strategies among oak species from central Mexico. *Tree Physiology* **37**: 915–925.

Allen CD, Macalady AK, Chenchouni H, Bachelet D, McDowell NG, Vennetier M, Kitzberger T, Rigling A, Breshears DD, Hogg EH *et al.* 2010. A global overview of drought and heat-induced tree mortality reveals emerging climate change risks for forests. *Forest Ecology and Management* **259**: 660–684.

Alon A, Cohen S, Burlett R, Eselson E, Riov J, Delzon S, David-Schwartz R. 2024. Leaf membrane leakage and xylem hydraulic failure define the point of no return in drought-induced tree mortality in *Cupressus sempervirens*. *Physiologia Plantarum* **176**: e14467.

Alpert P. 2006. Constraints of tolerance: why are desiccation-tolerant organisms so small or rare? *Journal of Experimental Biology* **209**: 1575–1584.

Andrade MT, Cardoso AA, Oliveira LA, Pereira TS, Haverroth EJ, Souza GA, DaMatta FM, Zsögön A, Martins SCV. 2024. Enhanced drought resistance in tomato via reduced auxin sensitivity: delayed dehydration and improved leaf resistance to embolism. *Physiologia Plantarum* **176**: e14408.

Anfodillo T, Di Bisceglie DP, Urso T. 2002. Minimum cuticular conductance and cuticle features of Picea abies and *Pinus cembra* needles along an altitudinal gradient in the Dolomites (NE Italian Alps). *Tree Physiology* **22**: 479–487.

Azzara M, Abate E, Chiofalo MT, Crisafulli A, Trifilo P. 2022. Delaying drought-driven leaf cells damages may be the key trait of invasive trees for ensuring their success in the Mediterranean basin. *Tree Physiology* **43**: 430–440.

Bajji M, Kinet J-M, Lutts S. 2002. The use of the electrolyte leakage method for assessing cell membrane stability as a water stress tolerance test in durum wheat. *Plant Growth Regulation* **36**: 61–70.

Baker NR. 2008. Chlorophyll fluorescence: A probe of photosynthesis *in vivo*. *Annual Review of Plant Biology* **59**: 89–113.

Bartlett MK, Zhang Y, Kreidler N, Sun S, Ardy R, Cao K, Sack L. 2014. Global analysis of plasticity in turgor loss point, a key drought tolerance trait. *Ecology Letters* **17**: 1580–1590.

Bi M, Jiang C, Yao G, Turner NC, Scoffoni C, Fang X. 2023. Rapid drought-recovery of gas exchange in *Caragana* species adapted to low mean annual precipitation. *Plant, Cell & Environment* **46**: 2296–2309.

Binks O, Meir P, Rowland L, da Costa ACL, Vasconcelos SS, de Oliveira AAR, Ferreira L, Mencuccini M. 2016. Limited acclimation in leaf anatomy to experimental drought in tropical rainforest trees. *Tree Physiology* **36**: 1550–1561.

Blackman CJ, Li X, Choat B, Rymer PD, De Kauwe MG, Duursma RA, Tissue DT, Medlyn BE. 2019. Desiccation time during drought is highly predictable across species of *Eucalyptus* from contrasting climates. *New Phytologist* **224**: 632–643.

Blackman CJ, Pfautsch S, Choat B, Delzon S, Gleason SM, Duursma RA. 2016. Toward an index of desiccation time to tree mortality under drought. *Plant, Cell & Environment* **39**: 2342–2345.

Bristiel P, Roumet C, Violle C, Volaire F. 2018. Coping with drought: root trait variability within the perennial grass *Dactylis glomerata* captures a trade-off between dehydration avoidance and dehydration tolerance. *Plant and Soil* **434**: 327–342.

Brodribb TJ, Jordan GJ, Carpenter RJ. 2013. Unified changes in cell size permit coordinated leaf evolution. *New Phytologist* **199**: 559–570.

Brodribb TJ, McAdam SAM, Jordan GJ, Martins SCV. 2014. Conifer species adapt to low-rainfall climates by following one of two divergent pathways. *Proceedings of the National Academy of Sciences, USA* **111**: 14489–14493.

Bueno A, Alfarhan A, Arand K, Burghardt M, Deininger A-C, Hedrich R, Leide J, Seufert P, Staiger S, Riederer M. 2019a. Effects of temperature on the cuticular transpiration barrier of two desert plants with water-spender and water-saver strategies. *Journal of Experimental Botany* **70**: 1613–1625.

Bueno A, Sancho-Knapik D, Gil-Pelegrín E, Leide J, Peguero-Pina JJ, Burghardt M, Riederer M. 2019b. Cuticular wax coverage and its transpiration barrier properties in *Quercus coccifera* L. leaves: does the environment matter? *Tree Physiology* **40**: 827–840.

Burghardt M. 2003. Ecophysiological relevance of cuticular transpiration of deciduous and evergreen plants in relation to stomatal closure and leaf water potential. *Journal of Experimental Botany* **54**: 1941–1949.

Burghardt M, Burghardt A, Gall J, Rosenberger C, Riederer M. 2008. Ecophysiological adaptations of water relations of *Teucrium chamaedrys* L. to the hot and dry climate of xeric limestone sites in Franconia (Southern Germany). *Flora* **203**: 3–13.

Burlett R, Trueba S, Bouteiller XP, Forget G, Torres-Ruiz JM, Martin-StPaul NK, Parise C, Cochard H, Delzon S. 2025. Minimum leaf conductance during drought: unravelling its variability and impact on plant survival. *New Phytologist* **246**: 14.

Cameron KD, Teece MA, Smart LB. 2006. Increased accumulation of cuticular wax and expression of lipid transfer protein in response to periodic drying events in leaves of tree tobacco. *Plant Physiology* **140**: 176–183.

Challis A, Blackman C, Ahrens C, Medlyn B, Rymer P, Tissue D, Martinez-Vilalta J. 2022. Adaptive plasticity in plant traits increases time to hydraulic failure under drought in a foundation tree. *Tree Physiology* **42**: 708–721.

Chen Z, Zhu S, Zhang Y, Luan J, Li S, Sun P, Wan X, Liu S. 2020. Tradeoff between storage capacity and embolism resistance in the xylem of temperate broadleaf tree species. *Tree Physiology* **40**: 1029–1042.

Christoffersen BO, Gloor M, Fauset S, Fyllas NM, Galbraith DR, Baker TR, Kruijt B, Rowland L, Fisher RA, Binks OJ *et al.* 2016. Linking hydraulic traits to tropical forest function in a size-structured and trait-driven model (TFS v.1-Hydro). *Geoscientific Model Development* **9**: 4227–4255.

Clarke JM, McCaig TN. 1982. Excised-leaf water retention capability as an indicator of drought resistance of *Triticum* genotypes. *Canadian Journal of Plant Science* **62**: 571–578.

Corso D, Delzon S, Lamarque LJ, Cochard H, Torres-Ruiz JM, King A, Brodribb T. 2020. Neither xylem collapse, cavitation, or changing leaf conductance drive stomatal closure in wheat. *Plant, Cell & Environment* **43**: 854–865.

Creek D, Lamarque LJ, Torres-Ruiz JM, Parise C, Burlett R, Tissue DT, Delzon S. 2020. Xylem embolism in leaves does not occur with open stomata: evidence from direct observations using the optical visualization technique. *Journal of Experimental Botany* **71**: 1151–1159.

Cutler JM, Rains DW, Loomis RS. 1977. The importance of cell size in the water relations of plants. *Physiologia Plantarum* **40**: 255–260.

Díaz-Castellanos A, Meave JA, Vega-Ramos F, Pineda-García F, Bonfil C, Paz H. 2022. The above–belowground functional space of tropical dry forest communities responds to local hydric habitats. *Biotropica* **54**: 1003–1014.

Ding YT, Zhang YX, Zheng QS, Tyree MT. 2014. Pressure-volume curves: revisiting the impact of negative turgor during cell collapse by literature review and simulations of cell micromechanics. *New Phytologist* **203**: 378–387.

Duursma RA, Blackman CJ, Lopéz R, Martin-StPaul NK, Cochard H, Medlyn BE. 2018. On the minimum leaf conductance: its role in models of plant water use, and ecological and environmental controls. *New Phytologist* **221**: 693–705.

Fallon B, Cavender-Bares J. 2018. Leaf-level trade-offs between drought avoidance and desiccation recovery drive elevation stratification in arid oaks. *Ecosphere* **9**: 25.

Forner A, Valladares F, Aranda I. 2018. Mediterranean trees coping with severe drought: avoidance might not be safe. *Environmental and Experimental Botany* **155**: 529–540.

Fortunel C, Stahl C, Coste S, Ziegler C, Derroire G, Levionnois S, Marechaux I, Bonal D, Herault B, Wagner FH *et al.* 2023. Thresholds for persistent leaf photochemical damage predict plant drought resilience in a tropical rainforest. *New Phytologist* **239**: 576–591.

Fradera-Soler M, Grace OM, Jorgensen B, Mravec J. 2022. Elastic and collapsible: current understanding of cell walls in succulent plants. *Journal of Experimental Botany* **73**: 2290–2307.

Grünhofer P, Herzig L, Zhang Q, Vitt S, Stöcker T, Malkowsky Y, Brügmann T, Fladung M, Schreiber L. 2023. Changes in wax composition but not amount enhance cuticular transpiration. *Plant, Cell & Environment* **47**: 91–105.

Guo Y, Ma Y, Ding C, Di N, Liu Y, Tan J, Zhang S, Yu W, Gao G, Duan J *et al.* 2023. Plant hydraulics provide guidance for irrigation management in mature polar plantation. *Agricultural Water Management* **275**: 108029.

Gupta A, Rico-Medina A, Caño-Delgado AI. 2020. The physiology of plant responses to drought. *Science* **368**: 266–269.

Holmlund HI. 2021. Synergistic adaptations: freezing tolerance is associated with desiccation tolerance and activation of violaxanthin de-epoxidase in wintergreen ferns. *Journal of Experimental Botany* **72**: 2814–2817.

Holtta T, Cochard H, Nikinmaa E, Mencuccini M. 2009. Capacitive effect of cavitation in xylem conduits: results from a dynamic model. *Plant, Cell & Environment* **32**: 10–21.

IPCC. 2023. *Climate change 2023: Synthesis report*. Geneva, Switzerland: Intergovernmental Panel on Climate Change.

John GP, Henry C, Sack L. 2018. Leaf rehydration capacity: associations with other indices of drought tolerance and environment. *Plant, Cell & Environment* **41**: 2638–2653.

Kerstiens G. 1996. Cuticular water permeability and its physiological significance. *Journal of Experimental Botany* **47**: 1813–1832.

Khoma Y, McAdam SAM. 2025. Tip-to-base conduit widening maintains hydraulic efficiency in aerial fern organs. *New Phytologist* **248**: 9.

Kramp RE, Liancourt P, Herberich MM, Saul L, Weides S, Tielbörger K, Májeková M. 2022. Functional traits and their plasticity shift from tolerant to avoidant under extreme drought. *Ecology* **103**: e3826.

Levitt J. 1980. *Responses of plants to environmental stresses*. New York, NY, USA: Academic Press.

Li X, He X, Smith R, Choat B, Tissue D. 2020. Temperature alters the response of hydraulic architecture to CO_2 in cotton plants (*Gossypium hirsutum*). *Environmental and Experimental Botany* **172**: 104004.

Liang X, Ye Q. 2024. Integrating dehydration tolerance and avoidance in drought adaptation. *Journal of Plant Ecology* **17**: rtae073.

Liu J, Carriquí M, Xiong D, Kang S. 2024a. Influence of IAA and ABA on maize stem vessel diameter and stress resistance in variable environments. *Physiologia Plantarum* **176**: e14443.

Liu J, Hochberg U, Ding R, Xiong D, Dai Z, Zhao Q, Chen J, Ji S, Kang S. 2023. Elevated CO_2 concentration increases maize growth under water deficit or soil salinity but with a higher risk of hydraulic failure. *Journal of Experimental Botany* **75**: 422–437.

Liu J, Huang J, Peng S, Xiong D. 2024b. Rewatering after drought: unravelling the drought thresholds and function recovery-limiting factors in maize leaves. *Plant, Cell & Environment* **47**: 5457–5469.

Lopez R, Cano FJ, Martin-StPaul NK, Cochard H, Choat B. 2021. Coordination of stem and leaf traits define different strategies to regulate water loss and tolerance ranges to aridity. *New Phytologist* **230**: 497–509.

Machado R, Loram-Lourenço L, Farnese FS, Alves RDFB, de Sousa LF, Silva FG, Filho SCV, Torres-Ruiz JM, Cochard H, Menezes-Silva PE. 2020. Where do leaf water leaks come from? Trade-offs underlying the variability in minimum conductance across tropical savanna species with contrasting growth strategies. *New Phytologist* **229**: 1415–1430.

Mantova M, Menezes-Silva PE, Badel E, Cochard H, Torres-Ruiz JM. 2021. The interplay of hydraulic failure and cell vitality explains tree capacity to recover from drought. *Physiologia Plantarum* **172**: 247–257.

Marks RA, Van Der Pas L, Schuster J, Gilman IS, VanBuren R. 2024. Convergent evolution of desiccation tolerance in grasses. *Nature Plants* **10**: 1112–1125.

Maxwell K, Johnson GN. 2000. Chlorophyll fluorescence-a practical guide. *Journal of Experimental Botany* **51**: 659–668.

Muchow RC, Sinclair TR. 1989. Epidermal conductance, stomatal density and stomatal size among genotypes of *Sorghum bicolor* (L.) Moench. *Plant, Cell & Environment* **12**: 425–431.

Nadal M, Brodribb TJ, Fernandez-Marin B, Garcia-Plazaola JI, Arzac MI, Lopez-Pozo M, Perera-Castro AV, Gulias J, Flexas J, Farrant JM. 2021. Differences in biochemical, gas exchange and hydraulic response to water stress in desiccation tolerant and sensitive fronds of the fern *Anemia caffrorum*. *New Phytologist* **231**: 1415–1430.

Nadal M, Clemente-Moreno MJ, Perera-Castro AV, Roig-Oliver M, Onoda Y, Gulias J, Flexas J. 2023. Incorporating pressure-volume traits into the leaf economics spectrum. *Ecology Letters* **26**: 549–562.

Oppenheimer HR, Leshem B. 1966. Critical thresholds of dehydration in leaves of *Nerium oleander* L. *Protoplasma* **61**: 302–321.

Pineda-Garcia F, Paz H, Meinzer FC. 2013. Drought resistance in early and late secondary successional species from a tropical dry forest: the interplay between xylem resistance to embolism, sapwood water storage and leaf shedding. *Plant, Cell & Environment* **36**: 405–418.

Proctor MCF, Tuba Z. 2002. Poikilohydry and homoihydry: antithesis or spectrum of possibilities? *New Phytologist* **156**: 327–349.

Raza S, Pandey BK, Hawkesford MJ, Griffiths S, Bennett MJ, Mooney SJ. 2025. Future crop breeding needs to consider future soils. *Nature Plants* **11**: 939–941.

Rehschuh R, Cecilia A, Zuber M, Faragó T, Baumbach T, Hartmann H, Jansen S, Mayr S, Ruehr N. 2020. Drought-induced xylem embolism limits the recovery of leaf gas exchange in scots pine. *Plant Physiology* **184**: 852–864.

Reich PB, Cornelissen H. 2014. The world-wide 'fast–slow' plant economics spectrum: a traits manifesto. *Journal of Ecology* **102**: 275–301.

Riederer M, Schreiber L. 2001. Protecting against water loss: analysis of the barrier properties of plant cuticles. *Journal of Experimental Botany* **52**: 2023–2032.

Samantara K, Ivandi E, Tulva I, Jalakas P, Doust BK, Ingver A, Kärp M, Brazauskas G, Bleidere M, Tamm I *et al.* 2025. Higher adaxial stomatal density is associated with lower grain yield in spring wheat. *New Phytologist* **248**: 454–460.

Sampangi-Ramaiah MH, Ravishankar KV, Seetharamaiah SK, Roy TK, Hunashikatti LR, Rekha A, Shilpa P. 2016. Barrier against water loss: relationship between epicuticular wax composition, gene expression and leaf water retention capacity in banana. *Functional Plant Biology* **43**: 492–501.

Sancho LG, Kappen L. 1989. Photosynthesis and water relations and the role of anatomy in Umbilicariaceae (lichenes) from Central Spain. *Oecologia* **81**: 473–480.

Schuster A-C, Burghardt M, Alfarhan A, Bueno A, Hedrich R, Leide J, Thomas J, Riederer M. 2016. Effectiveness of cuticular transpiration barriers in a desert plant at controlling water loss at high temperatures. *AoB Plants* **8**: plw027.

Scoffoni C, Chatelet DS, Pasquet-kok J, Rawls M, Donoghue M, Edwards EJ, Sack L. 2016. Hydraulic basis for the evolution of photosynthetic productivity. *Nature Plants* **2**: 16072.

Smith DC, Molesworth S. 1973. Lichen physiology XIII. Effects of rewetting dry lichens. *New Phytologist* **72**: 525–533.

Song Q, Zhu X-G. 2024. Techniques for photosynthesis phenomics: gas exchange, fluorescence, and reflectance spectrums. *Crop and Environment* **3**: 147–158.

Trifilo P, Abate E, Petruzzellis F, Azzara M, Nardini A. 2023. Critical water contents at leaf, stem and root level leading to irreversible drought-induced damage in two woody and one herbaceous species. *Plant, Cell & Environment* **46**: 119–132.

Trueba S, Pan R, Scoffoni C, John GP, Davis SD, Sack L. 2019. Thresholds for leaf damage due to dehydration: declines of hydraulic function, stomatal conductance and cellular integrity precede those for photochemistry. *New Phytologist* **223**: 134–149.

Turner NC. 1986. Adaptation to water deficits: A changing perspective. *Functional Plant Biology* **13**: 175–190.

Wagner Y, Volkov M, Nadal-Sala D, Ruehr NK, Hochberg U, Klein T. 2023. Relationships between xylem embolism and tree functioning during drought, recovery, and recurring drought in Aleppo pine. *Physiologia Plantarum* **175**: e13995.

Wang J, Mao L, Li Y, Lu K, Qu C, Tang Z, Li J, Liu L. 2024. Natural variation in *BnaA9.NF-YA7* contributes to drought tolerance in *Brassica napus* L. *Nature Communications* **15**: 2082.

Wang S, Hoch G, Grun G, Kahmen A. 2024. Water loss after stomatal closure: quantifying leaf minimum conductance and minimal water use in 9 temperate European tree species during a severe drought. *Tree Physiology* **44**: tpae027.

Wang X, Huang J, Peng S, Xiong D. 2023. Leaf rolling precedes stomatal closure in rice (*Oryza sativa*) under drought conditions. *Journal of Experimental Botany* **74**: 6650–6661.

Wright IJ, Reich PB, Westoby M, Ackerly DD, Baruch Z, Bongers F, Cavender-Bares J, Chapin T, Cornelissen JHC, Diemer M *et al.* 2004. The worldwide leaf economics spectrum. *Nature* **428**: 821–827.

Xiong D, Flexas J. 2020. From one side to two sides: the effects of stomatal distribution on photosynthesis. *New Phytologist* **228**: 1754–1766.

Zait Y, Shemer OE, Cochavi A. 2024. Dynamic responses of chlorophyll fluorescence parameters to drought across diverse plant families. *Physiologia Plantarum* **176**: e14527.

Zhu X, Xiong L. 2013. Putative megaenzyme DWA1 plays essential roles in drought resistance by regulating stress-induced wax deposition in rice. *Proceedings of the National Academy of Sciences, USA* **110**: 17790–17795.

Ziegler C, Cochard H, Stahl C, Foltzer L, Gérard B, Goret J-Y, Heuret P, Levionnois S, Maillard P, Bonal D *et al.* 2024. Residual water losses mediate the trade-off between growth and drought survival across saplings of 12 tropical rainforest tree species with contrasting hydraulic strategies. *Journal of Experimental Botany* **75**: 4128–4147.

Supporting Information

Additional Supporting Information may be found online in the Supporting Information section at the end of the article.

Dataset S1 The source data underlying Figs 1–4.

Fig. S1 The typical leaf dehydration curve, rehydration capacity loss curve, Chl fluorescence loss curve, and their critical values.

Fig. S2 The correlation analysis between leaf water retention capacity and Chl fluorescence retention capacity.

Fig. S3 Leaf anatomical and physiological traits associated with leaf water retention and rehydration capacities.

Fig. S4 Proportions of leaf types of selected species in different temperature zones.

Fig. S5 Comparisons of leaf mass per area between different leaf types.

Fig. S6 Comparisons of leaf Chl fluorescence retention capacity between different plant phyla, original biomes, growth forms, and leaf types.

Fig. S7 Correlations between leaf saturated water content and mesophyll porosity, leaf mass per area, and leaf thickness.

Fig. S8 The correlation analysis between leaf water retention capacity and the RWC at inflection point of conductance.

Table S1 List of abbreviations.

Table S2 Information of species used in this study.

Please note: Wiley is not responsible for the content or functionality of any Supporting Information supplied by the authors. Any queries (other than missing material) should be directed to the *New Phytologist* Central Office.